

Suspended Gold Nanowires: Ballistic Transport of Electrons

Kunio Takayanagi

Tokyo Institute of Technology, Graduate School of Interdisciplinary Science and Technology,
4259 Nagatuta, Midori-ku, Yokohama, 226-8502 Japan

Yukihito Kondo¹⁾ and Hideaki Ohnishi²⁾

Particle Surface Project of ERATO, JST,

Abstract

Gold nanowires a few atomic diameters wide are observed by ultra-high vacuum transmission electron microscopy, and their conductance measured simultaneously using a scanning tunneling microscope built into the electron microscope. A strand of gold atoms suspended between electrodes is directly observed to have a conductance of $2e^2/h$ ($=12.9 \text{ k}\Omega^{-1}$), where e is the electron charge and h is Planck's constant. This conductance quantization results from ballistic transport of electrons through a conduction channel of the strand.

1. Introduction

As the scale of microelectronic engineering continues to decrease, the nature of electron transport through one-dimensional nanometer-scale channels such as quantum wires¹⁾ and carbon nanotubes^{2,3)} has become important. Quantum point contacts (QPCs) are structures in which a "neck" of atoms a few atomic diameters wide bridges two electrodes. Metal QPCs were formed by connecting two metal electrodes using a scanning tunneling microscope (STM)⁴⁻⁷⁾ a mechanically controllable breaking junction (MCB)⁸⁻¹¹⁾ and relay switch¹²⁾ geometry. These QPCs typically display a stepwise conductance change as the contact is withdrawn, with a conductance step of $2e^2/h$, where e is the electron charge and h is Planck's constant.

A metal QPC's structure and conductance were directly observed by using an ultra-high-vacuum transmission electron microscope (UHV-TEM) which has a miniaturized STM at the specimen position. A gold nanowire formed between the gold STM tip and gold sample was directly observed by TEM at atomic resolution, with the conductance of the QPC measured simultaneously. The gold QPC showed conductance quantization with a step of $2e^2/h$ during withdrawal of the STM tip.¹³⁾ Gold nanowires have helical multi-shell structures, in which

strands of gold atoms are coiled around the axis of the nanowire.¹⁴⁾

2. Conductance quantization

Every material has a definite conductivity, so that the conductance of a wire is inversely proportional to the length of the wire. On the other hand, as the length scale of the wire is reduced to the mean free path of electrons, the electron transport mechanism changes from diffusive to ballistic, as shown in Fig. 1. When the width of the wire is further reduced to the nanometer or Fermi wavelength scale, the conductance between electrodes connected by the nanowire is quantized in steps of $2e^2/h$ ($=12.9$

$\text{k}\Omega^{-1}$). Moreover, the conductance is no longer dependent on the length of the wire. The conductance of a narrow constriction formed between two electrodes is generally understood by the Landauer formula:¹⁵⁾

$$G = (2e^2/h)\sum T_j, \quad (1)$$

where T_j is the electron transmission probability for the j -th conductance channel. Since $T_j=1$ for ballistic transport, $G=(2e^2/h)N$ for a nanowire (constriction) with N conduction channels.

Provided the constriction has width W , as shown in Fig. 1, the momentum p_x and p_y of the electron waves confined in the wire is quantized. The momentum is given by $hn/2W$, for

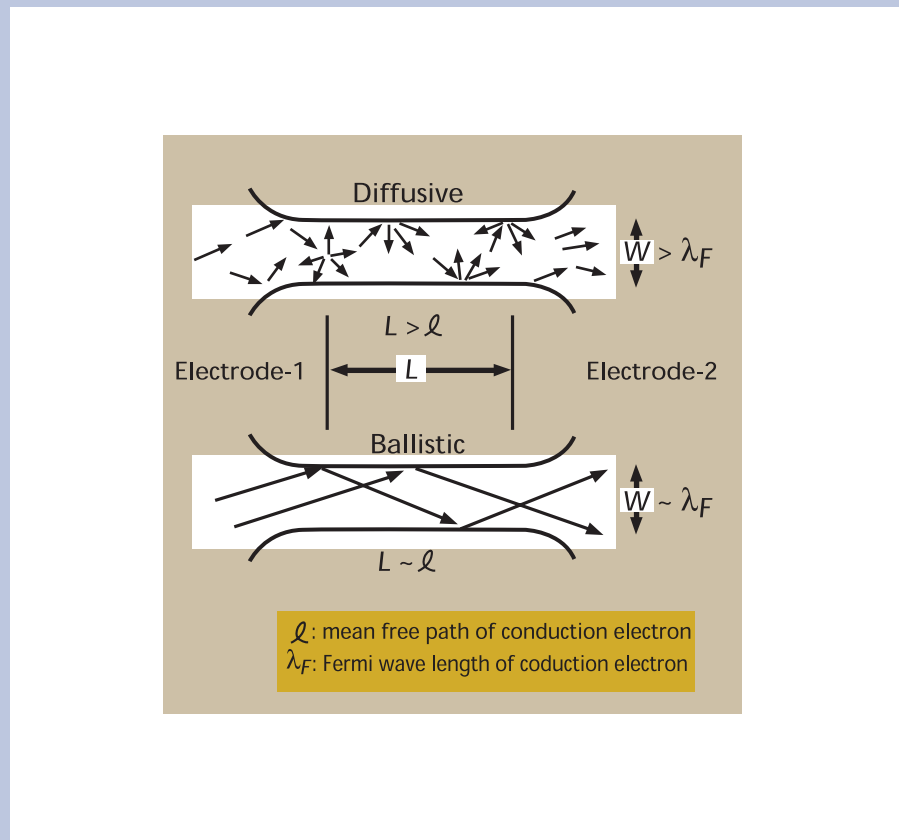


Fig. 1 Diffusive (a) and ballistic (b) transport of electrons in one-dimensional wires. l is the mean free path of the electrons, and λ_F is the Fermi wavelength.

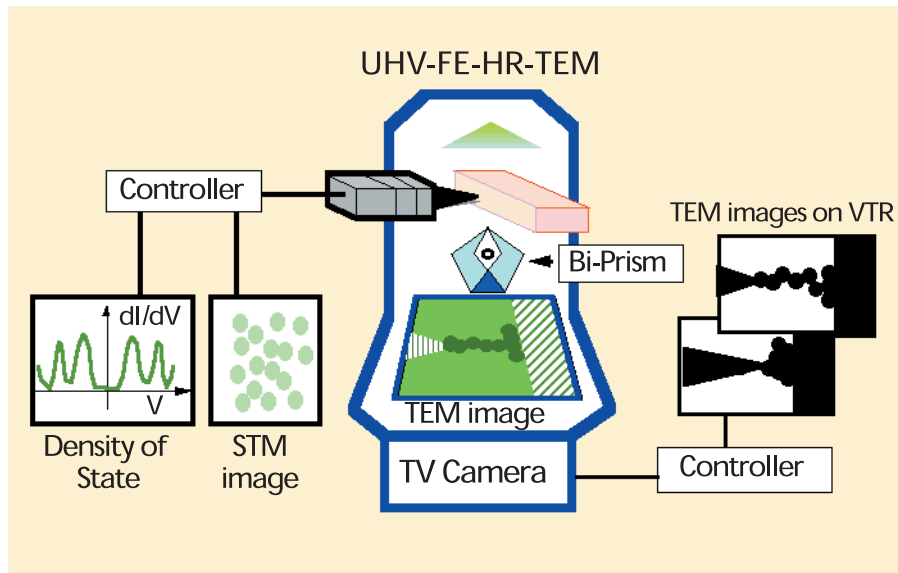


Fig. 2 STM-TEM instrument. A miniaturized scanning tunneling microscope (STM) is included at the specimen position of a UHV high-resolution transmission electron microscope (HR-TEM). A nanowire is formed between the gold STM tip and a gold substrate.

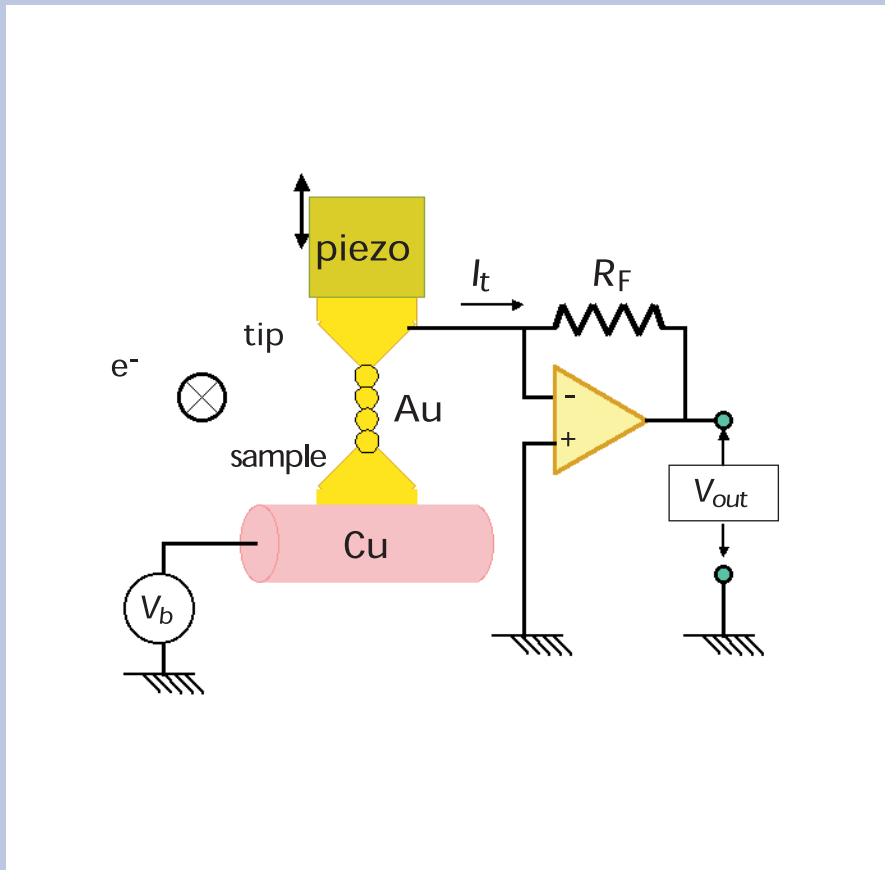


Fig. 3 Electronic circuit for measuring the conductance of a gold nanowire. A gold substrate deposited on a Cu rod and a gold STM tip are biased by V_b . The conduction current I_t is measured as $I_t = V_{out} / R_F$. The conductance between the electrodes (tip and sample) is calculated by $G = I_t / V_b$.

integral values of n . Then, electrons of energy E (mass m) can not be transported through the constriction if $p_z^2 = 2mE - (p_x^2 + p_y^2)$ is negative. The largest number of n defines the number of conduction channels N . N is determined so that the maximum p_x can not exceed h/λ_F , where λ_F is the Fermi wavelength of the electrons in the electrodes. For a potential difference of eV between the electrodes, electrons having energies from E_f to $E_f + eV$ contribute to the conduction current, where E_f is the Fermi energy. Taking spin degeneracy into account, then, $G = 2e^2/h$ is obtained for each conduction channel. The number of conduction channels depends on the width of the nanowire, so the conductance decreases stepwise as the nanowire is thinned.¹⁶⁾

Conductance quantization has been discussed theoretically more rigorously for atomic nanowires.¹⁷⁻¹⁹⁾ Transmission properties that depend on electron-electron interactions or spin degeneracy are interesting. The former reduces T_j ,²⁰⁾ while the latter produces the e^2/h conductance step.²¹⁾

3. UHV transmission electron microscope with built-in STM

Metal QPCs are made by withdrawing electrodes bridged by a nanowire. During the withdrawal, the nanowire is thinned and elon-

gated until it ruptures. The current passing between the electrodes under a constant bias voltage is used to measure the conductance step. Conductance changes are displayed on an oscilloscope for each withdrawal. Experiments are done progressively for a number of metals, such as Au, Ag, Cu, Pt, Al, Fe, Ni, Co, Bi, Pb, Hg, and Na. The conductance steps measured for many withdrawal experiments are displayed in histograms, whose peaks appeared at around Ne^2/h (where $N=1$ and 2), suggesting quantization of the conductance. The structure of these QPCs has not been examined except by computer simulation, however.

To simultaneously study structure and conductance, we developed a UHV high-resolution transmission electron microscope (HR-TEM) with a miniaturized STM at the specimen position, as shown schematically in Fig. 2. The UHV-HR-TEM was equipped with a field emission gun operated at 200 kV. Operating the UHV-HR-TEM at 10^{-8} Pa enabled clean fabrication of gold tips and samples in-situ, thereby eliminating any effects of contamination on the structure and conductance. A mechanically sharpened gold tip was brought close to a gold island that had been deposited on a very thin copper wire, as shown in Fig. 3. The gold tip was dipped into the gold island and then withdrawn by a shear-type piezoelectric transducer. The tip was withdrawn slowly, at a constant speed under computer control. Structural changes in the gold QPC were observed continuously during withdrawal by using a video monitor. The conductance of the gold QPC was measured simultaneously by the electrical connections shown in Fig. 3. The structure and conductance of the QPC were simultaneously recorded in each frame of the video images at 33-ms intervals.

4. Conductance and structure changes of gold nanowire

Successive structure and conductance changes of gold QPCs were observed using the STM-TEM. The structure of QPCs is dependent on the orientation of their electrodes. A QPC with electrodes oriented along the [110] crystalline axis is shown in Fig. 4, and the corresponding conductance is shown in Fig. 5. Figures 4(a)-(f) are electron microscope images during the withdrawal of the gold STM tip, and (002) lattice planes with a 0.2-nm spacing can be seen. The dark lines in the gold nanowire represent rows of gold atoms spanning the distance from the gold substrate to the tip. The nanowire thins in Figs. 4(a)-(e) and has ruptured

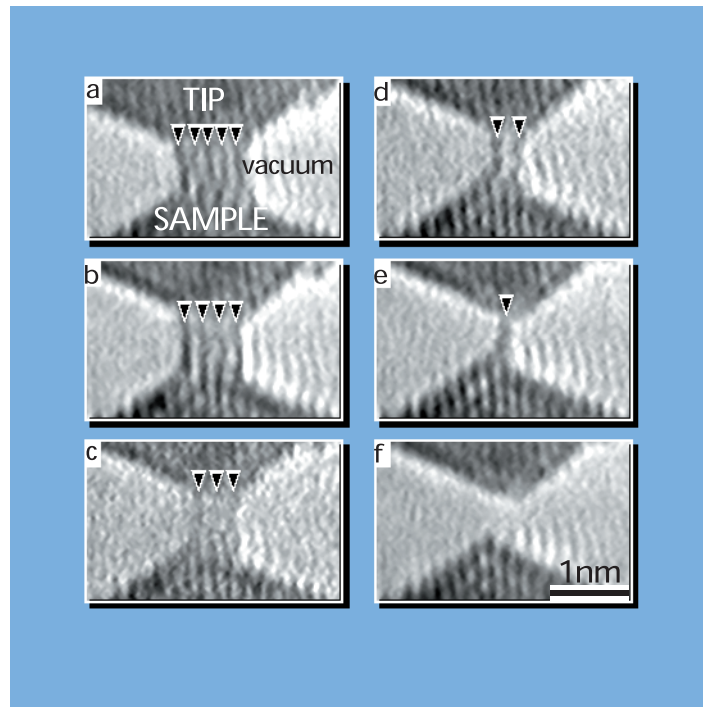


Fig. 4 Transmission electron microscope images of a gold nanowire during withdrawal. The tip and sample are oriented in the [110] direction, and the dark lines appearing in them are (002) lattice fringes spaced at 0.2 nm. The dark lines (or dark line) connecting the tip and sample are the nanowires.

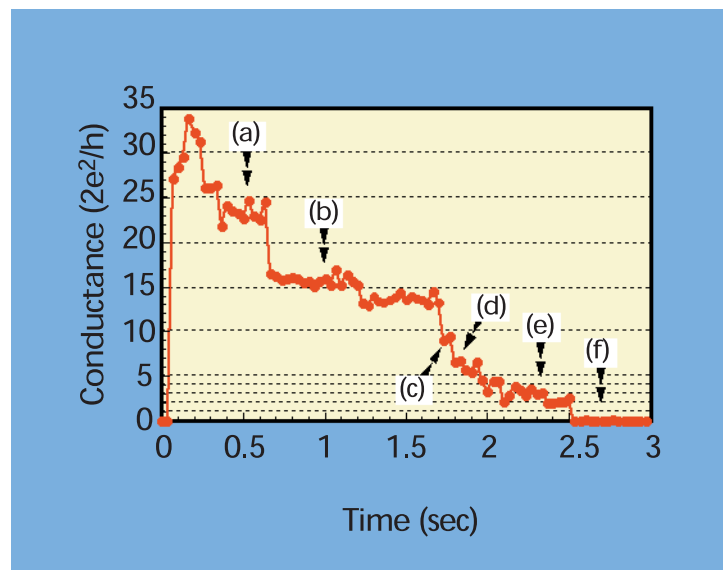


Fig. 5 Conductance steps observed for the withdrawal process shown in Fig. 4. The arrows labeled (a)-(f) show correspondence to images (a)-(f) in Fig. 4.

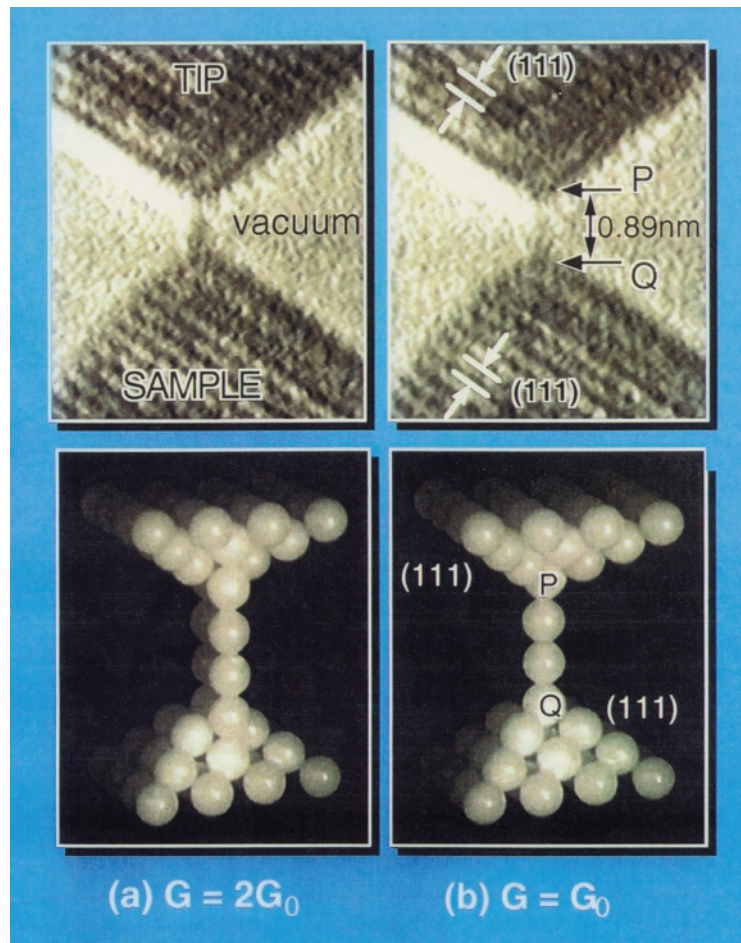


Fig. 6 Structural models of (a) a double strand and (b) a single strand of gold atoms, which span electrodes oriented in the [110] direction. The imaging electron beam is along the [1-10] direction. The distance between P and Q is 0.89 nm.

in Fig. 4(f). The dark lines disappear one-by-one, and at each disappearance the nanowire appears to be reorganized into a stable structure so that it maintains a regular and uniform diameter. The atomic structures of each nanowire have not been determined directly from these images. It is worth noting that the dark lines in Figs. 4(a)-(e) (especially in Fig. 4(e)) have an enlarged spacing relative to the (002) lattice spacing of the tip and substrate, which indicates that new structures formed at the nanowire (see the following section).

The conductance, shown in Fig. 5, changed stepwise in accordance with the structure changes shown in Fig. 4. The nanowire withdrawal steps shown in Figs. 4(a)-(f) thus correspond to the conductances labeled by arrows (a)-(f) in Fig. 5, with the conductance changing in steps of $n(2e^2/h)$. The plateaus in

Fig. 5 for each stable nanowire structure in Figs. 4(a)-(e) indicate one-to-one correspondence between the structure and the conductance. Scattering of the conductance values for each plateau follows any scattering of the local structure of the nanowire, or of the contact between the nanowire and the electrode.

More than 300 experiments provided clear evidence that a linear strand of gold atoms has a unit conductance of $G_0=2e^2/h$. Experiments also gave evidence that a double strand of gold atoms has a conductance twice the unit conductance. Figures 6(a) and (b) show structure models of the double strand and single strand, deduced from quantitative analysis of bright-dark image contrast like that in Fig. 4(e). Since the electrodes are in the [110] direction, each strand is coherent with the [110] atomic rows in the electrode bridges. Electron microscope

images, which gave a distance from P to Q as large as 0.89 nm, suggest that the gold atoms in the strand have the same nearest neighbor distance (0.29 nm) as in the bulk gold crystal. Thus, we verified that a QPC with [110] electrodes forms a nanowire at the contact, with the conductance quantized in steps of $N(2e^2/h)$ for each step of structural change in the nanowire.

5. Gold magic-nanowires suspended in vacuum

The structure of a gold QPC was studied at atomic resolution. A very thin gold film was placed on the specimen stage of the UHV-HR-TEM and bombarded with a very strong (~ 100 A/cm²) electron beam in order to bore holes in the film. As the holes were enlarged, a free-standing nanobridge of gold film was formed

in vacuum. By thinning the nanobridge further, it turned into a nanowire or into a single strand of atoms with a regular structure. The thinning process of the gold film and the formation of a nanowire or single atomic strand were recorded at atomic resolution, on videotape. These phenomena have never captured before.

Long gold nanowires could be formed in the [110] direction by using a gold (001) film, as shown in Fig. 7. The thinnest wire shown in Fig. 7(a) had a diameter (width) of around 0.6 nm. For each image, we can see wave-like lines along the wire axis (view the images from the wire axis at the grazing angle). These wave-like images can not be explained if the nanowires have a crystalline structure. After elaborate computer simulation based on these images, the gold nanowires were found to have helical multi-shell structures, as illustrated in Fig. 8. Each shell is tubular, made of atomic strands that coil around the axis of the tube, and characterized by the number of atomic strands. An L-M-N shell structure thus has three coaxial tubes, and the outermost tube has L atomic strands. The observed images were characterized as 7-1, 11-4, 13-6, and 14-7-1 multi-shell structures. The circumferences of the outer and inner tubes have a difference of $7d$ for all nanowires (d : lattice constant), indicating "magic number" of seven. Because of the odd magic number, gold nanowires must always have helical structures, so they have chirality similar to that of carbon nanotubes. Although

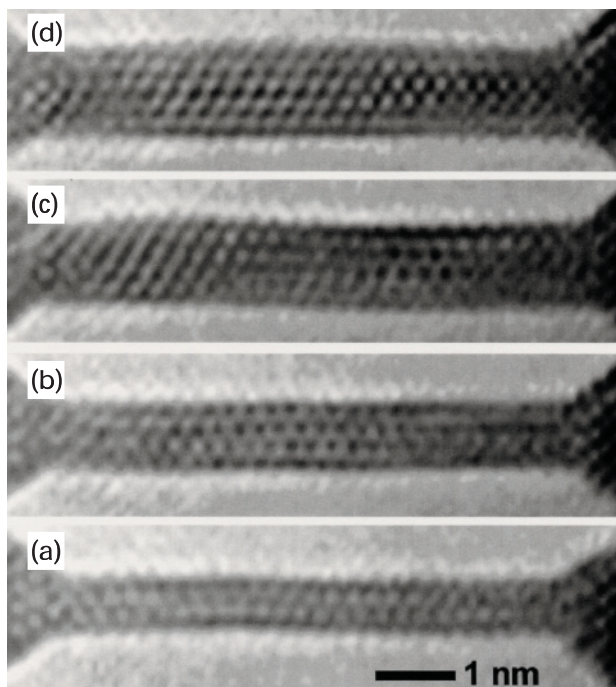


Fig. 7 Transmission electron microscope images of gold nanowires. The dark dots represent gold atoms. We view the images at the grazing angle from the wire direction. Note also the diameters of the nanowires: 1.3 nm, 1.1 nm, 0.8 nm, and 0.6 nm.

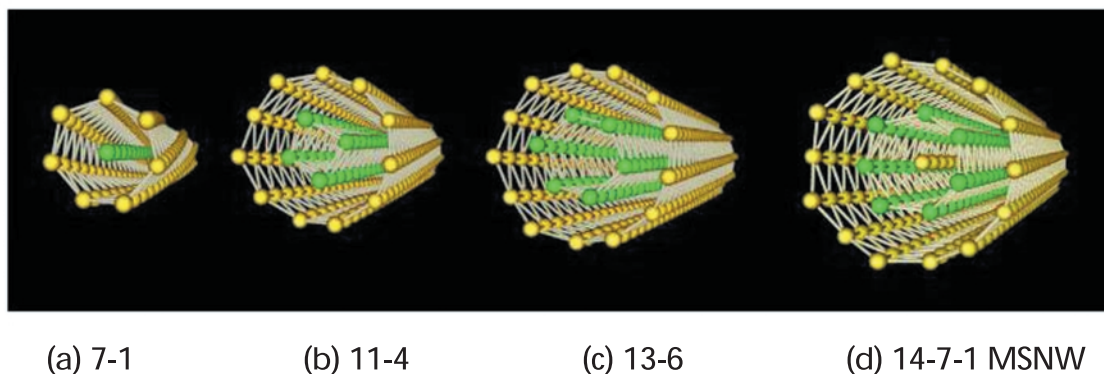


Fig. 8 Helical multi-shell structures of gold nanowires. Models (a) - (d) show the 7-1, 11-4, 13-6, and 14-7-1 structures. Each shell(tube) is helical and characterized by the number of atom strands (n). The n -fold helix of each shell is composed by a tube with triangular close-packed network of gold atom.

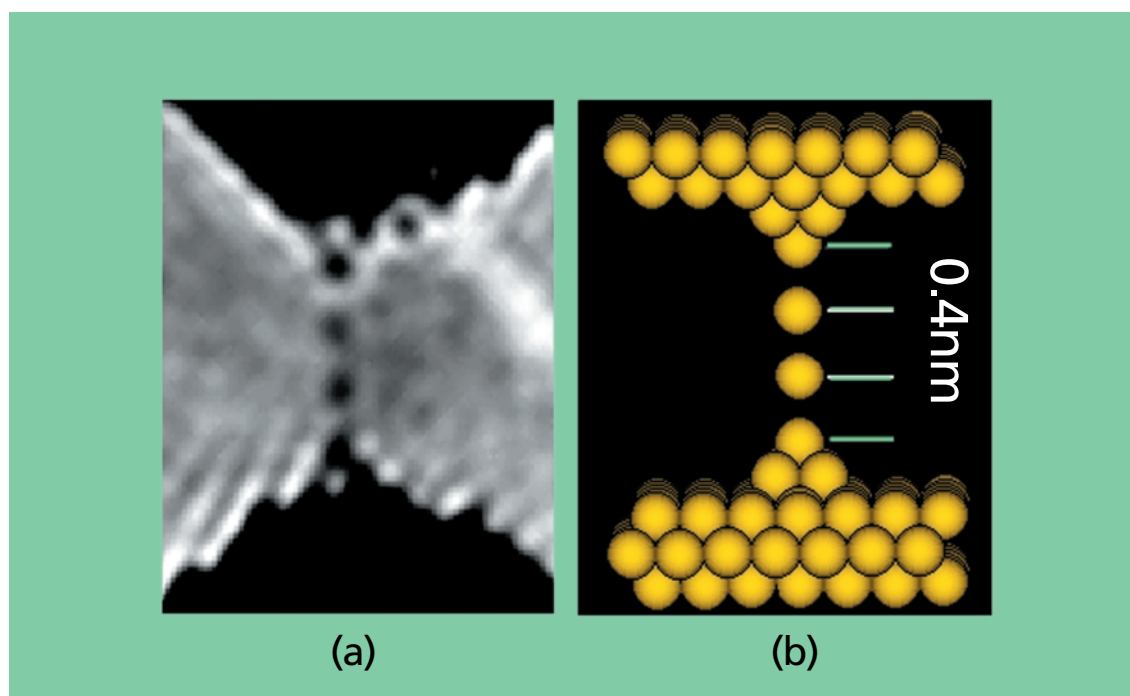


Fig. 9 Transmission electron microscope image (a) and model (b) of a single strand of gold atoms. The gold strand is in the [100] direction, and the imaging electron beam is along the [011] direction. Note that the gold atoms in the strand are spaced at approximately 0.4 nm.

we have not yet observed a single-shell gold nanowire, 6-0 and 5-0 single-shell structures are very likely to exist.

The thinnest nanowire is a single strand of atoms (a linear chain of atoms). Figure 9 shows an image of a single strand, which was made from a gold thin film of the (011) orientation. The strand extends along the [100] direction. This [100] strand contrasts with strands in the [110] direction, such as those shown in Fig. 7. The [100] strand in Fig. 9 has been elongated to have an inter-atomic distance of 0.4 nm, which is unexpectedly long compared with the nearest neighbor distance (0.29 nm at room temperature). A single strand of atoms which is suspended in vacuum (Fig.6b) has a conductance of $(12.9 \text{ k}\Omega)^{-1}$. Therefore, a single strand passes a current as large as $1 \mu\text{ A}$ with a bias voltage of 13 mV. High current density on the order of 10^7 A/mm^2 thus results from ballistic electron transport.

6. Quantum Architecture by Invisible

Conductance quantization of electrons passing through a narrow constriction was demonstrated not only for electrons, but also for QPCs in a two-dimensional electron gas (GaAs/GaAlAs) system.²²⁾ In both cases electron

transport is ballistic, since a nanowire has a width comparable to the Fermi wavelength and much shorter than the mean free path of electrons. Therefore, quantization of electronic conductance is common nature for all one-dimensional materials.

Because of ballistic transport, nanowires are thought to have zero resistance, with little energy dissipation such as Joule heating. In this respect, the quantization or quantum limit of thermal transport might become important,^{23, 24)} since it restricts heat dissipation from the system. As the scale of electronic circuits decreases further, we should encounter these quantum limits. One-dimensional nanowires displaying quantization of electron, phonon, and entropy transport should then play important and useful roles. Quantum architecture using nanoscale materials is an invisible world, but "there is plenty of room at the bottom" in such invisible world which will be realized in the 21 century.

Present address:

- 1) EMG Electron Optics Division JEOL LTD.
3-1-2, Musashino, Akishima, Tokyo 196-8558 JAPAN
- 2) Research Center for Ultra-High Voltage Electron Microscopy
Osaka University
7-1, Mihogaoka, Ibaraki, Osaka 567-0047, JAPAN

JSAP

References

- 1) R. A. Webb, S. Washburn, C. P. Umbach and R. B. Laibowitz: Phys. Rev. Lett. 54, 2696 (1985).
- 2) S. Iijima: Nature 354, 56 (1991).
- 3) M. Bockrath, et.al.: Science 275, 1922 (1997).
- 4) N. Agrait, J. G. Rodrigo and S. Vieira: Phys. Rev. B47, 12345 (1993).
- 5) J. L. Pascual, et al.: Science 267, 1793 (1995).
- 6) L. Olesen, et al.: Phys. Rev. Lett. 72, 2251 (1994).
- 7) J. L. Costa-Kramer, et al.: Phys. Rev. B55, 5416 (1997).
- 8) C. J. Muller, J. M. Krans, T. N. Todorov and M. A. Reed: Phys. Rev. B53, 1022 (1996).
- 9) U. Landman, W. D. Luedtke, B. E. Salisburly and R. L. Whetten: Phys. Rev. Lett. 77, 1362 (1996).
- 10) J. L. Costa-Kramer, N. Garcia, P. Garcia-Mochales and P. A. Serena: Surface Sci. 342, L1144 (1995).
- 11) K. Hansen, E. Laegsgaard, I. Stensgaard and F. Besenbacher: Phys. Rev. B56, 2208 (1997).
- 12) H. Yasuda and A. Sakai: Phys. Rev. B56, 1069 (1997).
- 13) H. Ohnishi, Y. Kondo and K. Takayanagi: Nature 395, 780 (1998).
- 14) Y. Kondo and K. Takayanagi: Science 289, 606 (2000).
- 15) R. Landauer: IBM J.Rev.Dev. 1, 223 (1957).
- 16) J.A.Torres and J. I. Saenz: Phys. Rev. Lett. 77, 2245 (1996).
- 17) N. D. Lang: Phys. Rev. B52, 5335 (1995).
- 18) K. Hirose and M. Tukada: Phys. Rev. B51, 5278 (1995).
- 19) M. Okamoto and K. Takayanagi: Phys. Rev. B60, 7808 (1999).
- 20) H. van Houten and C. Beenakker: Physics Today (1996).
- 21) H. Oshima and K. Miyano: Appl. Phys. Lett. 73, 2203 (1998).
- 22) B. J. van Wees, et al.: Phys. Rev. Lett. 60, 848 (1988).
- 23) K. Schwab, E. A. Henriksen, J. M. Worlock and M. L. Roukes: Nature 404, 974 (2000).
- 24) J. B. Pendry: J. Phys. A16, 2161 (1983).